Journal of Pharmacokinetics and Biopharmaceutics, Vol. 11, No. 5, 1983

An Understanding of the Role of Enzyme Localization of the Liver on Metabolite Kinetics: A Computer Simulation

K. Sandy Pang[1,3] and Richard N. Stillwell[2]

Received January 25, 1983—Final August 18, 1983

The metabolic sequence of drug, D, *to its primary* (MI) *and terminal* (MII) *metabolites as mediated by enzymes* A *and* B, *respectively, was chosen to illustrate metabolizing activities among hepatocytes in different regions of the liver lobule. Six models of distributions of the hepatocellular activities (intrinsic clearances for* A *and* B*) were defined with respect to the flow path in liver, and the concentrations* D, MI, *and* MII *in the liver were simulated. The extent of sequential metabolism of the primary metabolite was compared for these six models of enzymic distributions. It was found that when the average hepatic intrinsic clearances of* A *and* B *were high (almost complete extraction of both drug and primary metabolite during their single passage through the liver), the distributions of* A *and* B *were not important determinants of metabolite kinetics. By contrast, when the average hepatic intrinsic clearances of* A *and* B *were both low, the distributions of* A *and* B *exerted profound effects on metabolite kinetics. The sensitivity to enzymic distribution in this region, however, was difficult to assess due to difficulties in detecting low levels of* MI *and* MII. *The effects of enzymic distributions on metabolite disposition would be better detected in compounds (drug and metabolite) with intermediate extraction ratios.*

KEY WORDS: Uneven distribution of enzymatic activities; primary metabolite; formation and elimination; intrinsic clearance; metabolite kinetics; sequential metabolism; generated metabolite; preformed metabolite.

INTRODUCTION

It is well recognized that the distribution of drug metabolizing enzymes in a major metabolizing/excretion organ such as the liver plays a very

This work was supported by USPHS Grants GM-27323; by a Research Career Development Award AM-01028; by the Medical Research Council of Canada; Faculty Development Award, DG-262, 263 & 264 (KSP); and by a USPHS Grant GM-13901 (RNS).

[1]Faculty of Pharmacy, University of Toronto, Toronto, Ontario, Canada M5S 1A1.
[2]Institute for Lipid Research, Baylor College of Medicine, Houston, Texas 77030.
[3]Author to whom reprint requests and inquiries should be addressed: Dr. K. S. Pang, Faculty of Pharmacy, University of Toronto, 19 Russell St., Toronto, Ontario, Canada M5S 1A1.

0090-466X/83/1000-0451$03.00/0

important role in drug and metabolite kinetics in the pharmacokinetic profiles of these entities in the whole body. Yet this aspect has not been examined nor emphasized in the course of development of pharmacokinetic principles. Most approaches assume a perfusion limitation, such that the concentration in venous blood emerging from an organ is in equilibrium with that in the organ (1). The assumption is inherent in compartmental analysis for the description of mono-, bi-, or multiexponential decay of drug or metabolite in the body (2), and is also present in physiological modeling where each organ is viewed as a discrete compartment (3–5). The distributions of drug metabolizing activities are not relevant in these approaches, because the eliminating organs are considered as "well mixed" and operationally behave as such; drug and metabolite disposition follows as if the distribution of enzyme systems were evenly distributed.

Models on hepatic elimination have since emerged. A "parallel tube" (6) or "sinusoidal perfusion" model assuming a perfusion limitation and an even distribution of enzymes throughout the liver predicts a bidirectional interchange of substrate between blood and hepatocyctes, but not direct exchange among hepatocytes, resulting in an exponential decay of drug concentration along the flow path in the liver. This model contrasts with the more frequently used model on hepatic elimination that is based on the assumption that the liver is an effectively "well-mixed" organ (7), and that the concentration in hepatic venous blood is in equilibrium with that in the organ.

The predictive properties of both models have been demonstrated: the "well-stirred" model was adequate in the prediction of the kinetics of lidocaine and its deethylated metabolite, MEGX (8,9), phenytoin (10), and propranolol (10), in the perfused rat liver preparation; the "parallel tube" model was accurate in the predictions of the elimination kinetics of galactose (11,12) and ethanol (13) in perfused liver preparations. When these models were further extended to describe the sequential metabolism of acetaminophen as a generated metabolite of phenacetin, a reaction sequence that entails O-deethylation followed by sulfation, both models failed to describe the kinetic phenomenon of sequential first-pass metabolism of the primary metabolite, acetaminophen, in the perfused rat liver preparation (14,15). Moreover, the extent of sulfation of the generated metabolite, acetaminophen, was significantly lower than the extent of sulfation of the *preformed metabolite*, that is, when acetaminophen was given as itself to the liver. The observed extent of acetaminophen sulfation lay halfway between the predictions of the "well-stirred" model, which predicts identical extents of sulfation for the generated and preformed metabolites, and the "parallel tube" model, which predicts a lesser extent of sulfation for the generated metabolite with respect to the preformed metabolite (14).

These data served as an incentive to probe the failure of both models in the prediction of metabolite kinetics. In sequential metabolism, two enzyme systems are involved: one for formation and one for metabolism of the generated metabolite. Failure of the above models in their predictions on acetaminophen sulfation when phenacetin was administered has been attributed to the preferential localization of drug metabolizing activities for O-deethylation and sulfation. O-deethylation occurs preferentially in the centrilobular region of the liver, or a region where sinusoidal blood drains out of the liver, whereas sulfation enzymes are enriched in the periportal region, or a region which receives the mixed supply of portal venous and hepatic arterial blood at the entrance of the flow path in the liver (16). These distribution patterns have also been well characterized by histochemical, morphometric, immunocytochemical, and staining techniques (17–19), as well as indirectly by induction (20) and inhibition (21) studies where toxicity served as an endpoint and indicated the presence of the enzyme systems.

Yet this phenomenon of uneven distribution of drug metabolizing enzymes within an organ such as the liver is often ignored in the treatment of (primary) metabolite kinetics, that is, the extent of sequential first-pass metabolism of the generated metabolite is usually considered as identical to the extent of metabolism of a preformed metabolite. In other words, the "well-stirred" model holds true. Also, there is a lack of understanding of the role of enzymatic activity for the formation of a primary metabolite on sequential metabolism. Again, the sequential first-pass metabolism of the generated metabolite is generally considered to be identical to the extent of metabolism of the preformed metabolite regardless of how rapidly the generated metabolite is formed; this assumption is inherent in the "well-stirred" model. It has only recently been demonstrated that the enzymatic activity for the formation of the primary metabolite is of paramount importance in determining the extent of sequential metabolism of the generated metabolite. The higher the enzymatic activity for formation of the primary metabolite, the more rapid will be the sequential elimination of the generated metabolite; the converse also holds true (22). Once-through liver perfusion studies with acetanilide, a slow-forming precursor of acetaminophen, and phenacetin, a fast-forming precursor of acetaminophen, have alluded to this kinetic observation (22). The extent of sequential metabolism of the generated metabolite will only equal that for the preformed metabolite at best, that is, when the generated metabolite is formed extremely rapidly in comparison to its sequential metabolism (23).

The consequences of the oversight on deviations of sequential metabolism of a generated metabolite form the metabolism of a preformed metabolite is an over-estimation of the extent of metabolism (or elimination)

of the generated metabolite. The severity of the error depends not only on the distribution of enzymic activities for primary metabolite formation and metabolism, but also on the relative enzymic activities for primary metabolite formation and metabolism.

The present communication describes a computer-assisted simulation for six models of enzymic distributions for the metabolic sequence of drug (*D*) that forms solely a primary metabolite (*MI*), which is further metabolized to a terminal metabolite (*MII*). Essentially, a tubular flow model is assumed, that is, bulk flow through the liver occurs through a common flow path and accounts for the majority of flow through the liver. The distribution of enzymes is varied and described with respect to this flow path.

The intent of the simulation is to (a) determine the pattern of enzymic distribution which is the least or the most efficient for sequential metabolism of *MI*, and (b) to identify conditions whereby the extent of sequential metabolism of *MI* is the least or the most sensitive to patterns of enzymic distributions. Identification of these factors will aid in the understanding of deviations of metabolite kinetics that arise during parent drug administration in comparison to the administration of a preformed primary metabolite.

THEORY

Several basic assumptions are made in the simulations. For the sake of clarity and simplicity, a condition similar to the once-through liver perfusion system is described, in which a constant input concentration of the drug *D*, C_{in}, is delivered under constant hepatic blood flow rate *Q* into the liver, and where steady-state output concentration of drug C_{out}, primary metabolite [*MI*], and terminal metabolite [*MII*] are detected in hepatic venous blood. The rate of drug and metabolite removal under steady-state conditions is attributable only to metabolism; binding is essentially completed and does not contribute to loss of drug and metabolites, and biliary excretion for drug and metabolite is nonexistent. The *average* intrinsic clearance for the formation and metabolism of the primary metabolite, mediated by enzymes *A* and *B*, respectively, are designated as $CL_{int,A}$ and $CL_{int,B}$. Several basic assumptions are taken:

1. Linear conditions are assumed; CL_{int} is the ratio of V_{max}/K_m (24,25).
2. The degree of binding of drug and metabolites to blood components remains constant along the entire flow path in liver.
3. The unbound species is that which is metabolized.
4. The rate of metabolism of each species is equal to the product of the CL_{int} and unbound concentration.

5. The *average* intrinsic clearance, or the area of the plot of intrinsic clearance and the length of flow path, L, is held constant in the comparison of the patterns of enzymic distributions; that is, although the intrinsic clearance varies along any point, x, within the flow path among the models, the time-averaged intrinsic clearance is held constant, i.e.,

$$CL_{int} = \int_0^L CL_{int,x} \cdot dx/L$$

The following mass balance differential equations are used in the description of the concentrations of drug and its metabolites in the flow path. The concentrations of these species at the end of the flow path, or L, becomes the hepatic venous concentrations:

$$-QdC_x = \frac{dx}{L} f_B C_x CL_{int,A_x} \tag{1}$$

$$QdC_x(MI) = \frac{dx}{L} f_B C_x CL_{int,A_x} - \frac{dx}{L} f_B(MI) CL_{int,B_x} \tag{2}$$

$$QdC_x(MII) = \frac{dx}{L} f_B(MI) C_x CL_{int,B_x} \tag{3}$$

where C_x, $C_x(MI)$, and $C_x(MII)$ are the concentrations of drug, primary, and terminal metabolites, respectively, along any point x of the flow path of length L; f_B and $f_B(MI)$, respectively, denote the unbound fractions of drug and primary metabolite in blood. CL_{int,A_x} and CL_{int,B_x} represent the hepatic intrinsic clearances for enzymes A and B at any point x along the flow path, and are described by the following relationships:

$$CL_{int,A_x} = CL_{int,A0} + \text{slope } A(x - A0) \tag{4}$$

$$CL_{int,B_x} = CL_{int,B0} + \text{slope } B(x - B0) \tag{5}$$

where $CL_{int,A0}$ and $CL_{int,B0}$, respectively, denote the initial values for the intrinsic clearances of A and B, respectively, at points $A0$ and $B0$ where the distributions of A and B commence. The points where the distributions of A and B end, however, are denoted by $A1$ and $B1$, respectively. When $A0 < x < A1$ and $B0 < x < B1$, CL_{int,A_x} and CL_{int,B_x} are described by Eqs. (4) and (5), respectively. For other conditions, these values are set as zero. $A0$, $B0$, $A1$, and $B1$ are distances within the flow path, L, and away from the point of entry of blood, which is designated as 0.

METHODS

Modeling studies were carried out on a PDP 11/45 computer with a program written in FORTRAN, with use of the GASP IV simulation package (26). The simulation package performs Runge–Kutta England (RKE) integrations of Eqs. (1)–(3), and at suitable intervals (1/1000 of the flow path), writes out the values of the variables representing the concentrations of the drug and its primary and terminal metabolites to disk files. These files are subsequently read by a general data plotting program (LSQ) and converted to plot files, which are then output to a Versatec printer-plotter. The hepatic venous concentrations of D, MI and MII (at L) are read after exiting the general program by the editing language TECO.

Although the equations contain more than one variable, e.g., C_x, CL_{int,A_x}, $C_x(MI)$, CL_{int,B_x}, $C_x(MII)$, and x, the intrinsic clearances are defined by Eqs. (4) and (5), and the concentrations may also be determined according to these values for the intrinsic clearances (Eqs. 1–3). The values for $CL_{int,A0}$, slope A, $A0$, $A1$, $CL_{int,B0}$, slope B, $B0$, and $B1$ are predetermined in the following fashion among the six models for enzymic distributions as shown in Fig. 1. In model I, the activity of A, CL_{int,A_x} increases

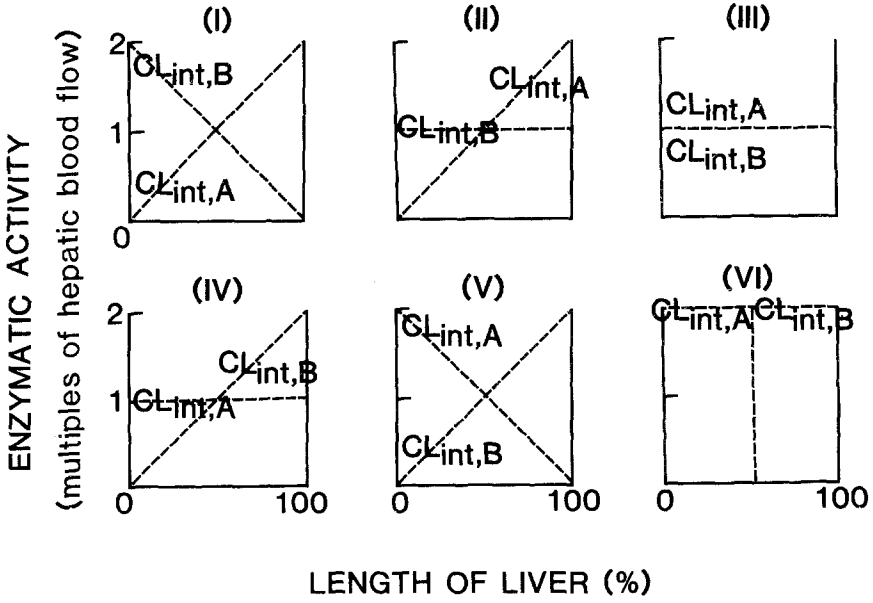

Fig. 1. Patterns of distributions of enzymes A and B among the six models. The average intrinsic clearance for enzymes A and B, $CL_{int,A}$ and $CL_{int,B}$, respectively, are equal to hepatic blood flow rate. See Table I for the assignment of the slopes and intercepts along the length of the flow path, L.

linearly from zero along the flow path, whereas that for B, CL_{int,B_x} decreases linearly to zero along the flow path. In model II, the distribution of A is the same as in model I, but the activity of B is evenly distributed. In model III, both activities for A and B are evenly distributed. In model IV, A is evenly distributed whereas the activity for B increases linearly from zero along the flow path. In model V, the activity of A decreases linearly to zero, but that for B increases linearly from zero along the flow path. In model VI, the distributions of A and B are evenly distributed, but A is not present in the second half of the liver, while B is absent in the first half of the liver. Another model which we have not shown describes the enzymic distributions of A and B as in model VI, but with the distributions for A and B reversed. For the sake of convenience, the flow path, L, is set as unity. The drug and its metabolites are unbound to blood components ($f_B = f_B(MI) = 1.0$), and the intrinsic clearances are expressed in terms of hepatic blood flow, Q. For the time-averaged intrinsic clearance for enzymes A and B equal to hepatic blood flow, the parameters which describe the enzymic distributions of A and B are shown in Table I.

The *average* intrinsic clearances for A and B, as defined earlier, are the plots of the areas of $CL_{int,x}$ for enzymes A and B, respectively, along the length of the liver. These are expressed in terms of hepatic blood flow rate: at high average intrinsic clearance (greater or equal to 10-fold flow), hepatic extraction ratio or E approaches unity; at intermediate average intrinsic clearance (equal to flow), the hepatic extraction ratio equals 0.632; at low average intrinsic clearances (0.1 times flow), the hepatic extraction ratio is less than 0.1.

Six sets of simulations were performed for each model (Fig. 1): (i) when the average intrinsic clearances of both A and B are high; (ii) when the average intrinsic clearance of A is intermediate and the average intrinsic clearance of B is varied; (iii) when the average intrinsic clearance of A is low, and the average intrinsic clearance of B is varied; (iv) when the average

Table I. Parameters Which Define the Distributions for Enzymes A and B When Their Respective Average Hepatic Intrinsic Clearances Equal That of Hepatic Blood Flow Rate[a]

Models	$CL_{int,A0}$ [b]	slope A	$A0$	$A1$	$CL_{int,B0}$ [b]	slope B	$B0$	$B1$
I	0	2	0	1	2	−2	0	1
II	0	2	0	1	1	0	0	1
III	1	0	0	1	1	0	0	1
IV	1	0	0	1	0	2	0	1
V	2	−2	0	1	0	2	0	1
VI	2	0	0	0.5	2	0	0.5	1

[a]The length of the flow path in liver is taken as unity.
[b]Multiples of hepatic blood flow rate, Q.

intrinsic clearance of B is high, and the average intrinsic clearance of A is varied; (v) when the average intrinsic clearance of B is intermediate, and the average intrinsic clearance of A is varied; (vi) when the average intrinsic clearance of B is low, and the average intrinsic clearance of A varied.

The calculations for the hepatic extraction ratio of drug is by the relationship:

$$E = \frac{C_{in} - C_{out}}{C_{in}} \tag{6}$$

The extent of sequential metabolism of the primary metabolite is assessed by the ratio of the output concentration of the terminal metabolite, $[MI]$, divided by the sum of the output concentrations for the primary and terminal metabolites, $[MI]+[MII]$.

RESULTS

High Average Intrinsic Clearances of *A* and *B*

Average intrinsic clearances of A and B are both high when the extraction ratio of drug and administered or preformed metabolite approaches 1. When the average intrinsic clearances of A and B were 10 times hepatic blood flow, the drug (D) disappeared rapidly in liver, and little accumulation of the primary metabolite (MI) occurred, due to its fast metabolism by enzyme B to form the terminal metabolite (MII). An example was provided by model I (Fig. 2a), which was the least efficient for sequential metabolism of MI among all models, because the majority of the enzymatic activity of B was present before that of A. Nonetheless, in this efficient model, the extent of sequential metabolism of the generated metabolite was almost complete, and was similar in value to that of the administered metabolite. In the model where enzyme B was present before A (model not shown on Fig. 1), no sequential metabolism of the generated metabolite occurred at any time because there was no overlap between enzymes A and B, and all of enzyme A was present posterior to enzyme B; the preformed metabolite, however, was metabolized (extraction ratio approaches 1).

On varying the average intrinsic clearance of B while keeping the average intrinsic clearance of A constant at 10 times hepatic blood flow (the ratio of $CL_{int,B}/CL_{int,A}$ was varied from 2500 to 0.1-fold), the sequential metabolism of MI was essentially complete when the average intrinsic clearance of B remained substantial (10 times hepatic blood flow); but when the average intrinsic clearance of B was only 0.1-fold of A (equal to hepatic blood flow), the extent of sequential metabolism of MI was much

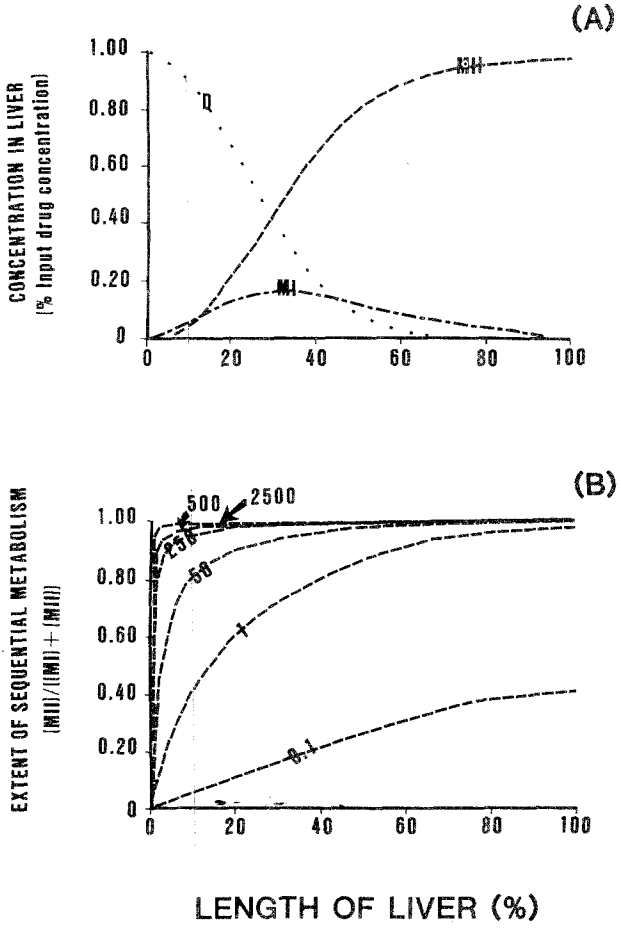

Fig. 2. (a) Simulated concentrations of drug (*D*) and primary (*MI*) and terminal (*MII*) metabolites in liver for model I when the average hepatic intrinsic clearances of *A* and *B* were set at 10 times hepatic blood flow rate (see text for details). (b) The extent of sequential metabolism of a generated primary metabolite for the six models of enzymic distributions when the ratio of the average intrinsic clearances of *B*/*A* were 2500, 500, 250, 50, 1, and 0.1; $CL_{int,A}$ was equal to 10 times hepatic blood flow rate.

less than unity (Fig. 2b). This trend was also consistent in other models presented (Models I to VI; Fig. 3). It appeared, therefore, that when the average intrinsic clearances of *A* and *B* were both very high (greater than 10 times hepatic blood flow), the enzymic distributions of *A* and *B* in liver became unimportant in the extent of metabolism of *MI*. By contrast, when

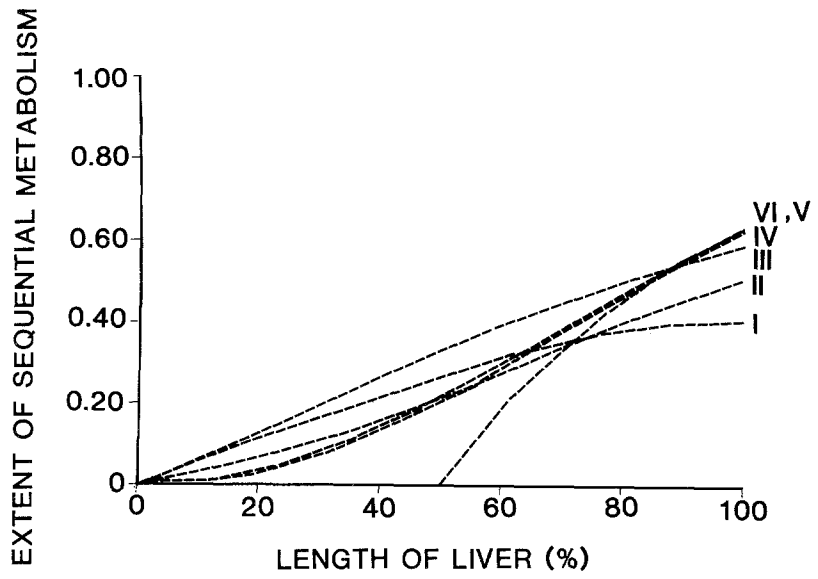

Fig. 3. The extent of sequential metabolism of a generated primary metabolite for the six models of enzymic distributions when the ratio of the average intrinsic clearances of B/A was 0.1; $CL_{int,A}$ was equal to 10 times hepatic blood flow rate.

the average intrinsic clearance of B was lower, enzymic distributions of A and B emerged as an important determinant (Fig. 3).

Among the six models on enzymic distributions, wide variations in the extent of metabolism of *MI* were seen when the ratio of B/A was 0.1 (Fig. 3). The order of increasing efficiency of the models for sequential metabolism of *MI* was from model I to model VI. In model VI, the primary metabolite was formed at the front half of the liver with further metabolism in the second half of the flow path, and there is no region where both A and B were present simultaneously (Fig. 1). For this very efficient model, the extent of metabolism of the generated metabolite would be equal to the extent of metabolism of the administered or preformed metabolite.

Sequential Metabolism of *MI* at Intermediate and Low Average Intrinsic Clearances of *A*

The sensitivity of the extent of metabolism of *MI* to varying average intrinsic clearances of B (50–0.1-fold of A) and to the enzymic distributions, when the average intrinsic clearance of A was intermediate (equal to hepatic blood flow with an extraction ratio of 0.632) or low (0.1 times hepatic blood flow with an extraction ratio of 0.0952) among the models is summarized in Table II. A comparison of the extent of sequential metabolism of

Table II. The Role of Average Intrinsic Clearances for Formation of Metabolite ($CL_{int,A}$) and Its Metabolic Intrinsic Clearance ($CL_{int,B}$) on the Extent of Sequential Metabolism

Average intrinsic clearances (multiples of Q)		Extent of sequential metabolism of primary metabolite models of enzymic distributions of A and B						Extraction ratio of drug	Extent of metabolism of preformed metabolite (extraction ratio)
Enzyme A	Enzyme B	I	II	III	IV	V	VI		
1	50	0.844	0.976	0.988	0.994	1.000	1.0	0.632	1.0
1	10	0.641	0.875	0.935	0.967	0.996	1.0	0.632	1.0
1	4	0.452	0.697	0.816	0.892	0.957	0.982	0.632	0.982
1	2	0.301	0.499	0.632	0.732	0.815	0.865	0.632	0.865
1	1	0.179	0.311	0.418	0.506	0.578	0.632	0.632	0.632
1	0.5	0.099	0.176	0.245	0.305	0.353	0.394	0.632	0.394
1	0.25	0.052	0.094	0.133	0.168	0.197	0.221	0.632	0.221
0.1	5	0.417	0.687	0.808	0.889	0.968	0.993	0.0952	0.993
0.1	1	0.142	0.269	0.373	0.467	0.558	0.632	0.0952	0.632
0.1	0.4	0.064	0.123	0.179	0.231	0.283	0.330	0.0952	0.330
0.1	0.2	0.033	0.065	0.095	0.125	0.154	0.181	0.0952	0.181
0.1	0.1	0.017	0.033	0.049	0.065	0.080	0.095	0.0952	0.095
0.1	0.05	0.009	0.017	0.025	0.033	0.041	0.049	0.0952	0.049
0.1	0.025	0.004	0.008	0.013	0.017	0.021	0.025	0.0952	0.025

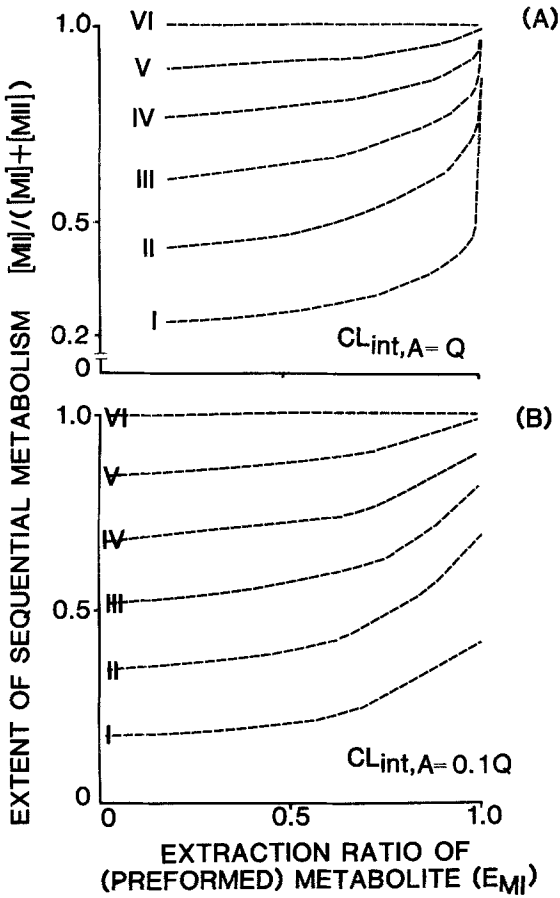

Fig. 4. The relationship between the extent of sequential metabolism of a generated primary metabolite and the extraction ratio of the preformed primary metabolite (E_{MI}) for the six models of enzymic distribution for average intrinsic clearances of A at (a) 1.0 and (b) 0.1 times hepatic blood flow rate.

the generated *MI* with the extent of metabolism of preformed *MI* was also afforded pictorially (Fig. 4). At constant intermediate average intrinsic clearance of A, differences in the extent of sequential metabolism among the models were seen (Fig. 4a); the line of zero slope for model VI virtually represented the behavior for the extent of metabolism of the preformed metabolite. At low average intrinsic clearance of A, more differences in the extent of sequential metabolism were observed (Fig. 4b). At both low average intrinsic clearances of A and B, the differences among the models were most marked (Fig. 4).

Table III. The Role of Average Intrinsic Clearances for Formation of Metabolite ($CL_{int,A}$) and its Metabolic Intrinsic Clearance ($CL_{int,B}$) on the Extent of Sequential Metabolism

Average intrinsic clearances (multiples of Q)		Extent of sequential metabolism of primary metabolite models of enzymic distributions of A and B						Extraction ratio of drug	Extent of metabolism of preformed metabolite
Enzyme A	Enzyme B	I	II	III	IV	V	VI		
500	10	1.000	1.000	1.000	1.000	1.000	1.0	1.0	1.0
100	10	1.000	1.000	1.000	1.000	1.000	1.0	1.0	1.0
50	10	0.999	1.000	1.000	1.000	1.000	1.0	1.0	1.0
10	10	0.973	0.997	1.000	1.000	1.000	1.0	1.0	1.0
1	10	0.641	0.875	0.935	1.000	1.000	1.0	0.632	1.0
0.5	10	0.591	0.849	0.919	0.995	0.995	1.0	0.394	1.0
0.1	10	0.550	0.826	0.904	0.994	0.994	1.0	0.095	1.0
50	1	0.534	0.582	0.625	0.632	0.632	0.632	1.0	0.632
10	1	0.405	0.508	0.591	0.624	0.630	0.632	1.0	0.632
5	1	0.319	0.444	0.546	0.601	0.622	0.632	0.993	0.632
1	1	0.179	0.311	0.418	0.506	0.578	0.632	0.632	0.632
0.1	1	0.142	0.269	0.373	0.467	0.558	0.632	0.095	0.632
0.05	1	0.140	0.267	0.370	0.464	0.557	0.632	0.049	0.632
0.01	1	0.139	0.264	0.368	0.462	0.556	0.632	0.010	0.632
5	0.1	0.040	0.059	0.077	0.089	0.093	0.095	0.993	0.095
1	0.1	0.021	0.039	0.056	0.072	0.084	0.095	0.632	0.095
0.5	0.1	0.019	0.035	0.052	0.068	0.082	0.095	0.394	0.095
0.1	0.1	0.017	0.033	0.049	0.065	0.080	0.095	0.095	0.095
0.01	0.1	0.016	0.033	0.048	0.084	0.080	0.095	0.010	0.095
0.005	0.1	0.016	0.033	0.048	0.064	0.080	0.095	0.005	0.095
0.001	0.1	0.016	0.033	0.048	0.064	0.080	0.095	0.001	0.095

Sequential Metabolism of *MI* at High, Intermediate, and Low Average Intrinsic Clearances of *B*

The sensitivity of the extent of sequential metabolism of *MI* to varying average intrinsic clearances of *A* (50 to 0.1-fold of *B*) and to enzymic distributions for high, intermediate, or low average intrinsic clearances of *B* is summarized in Table III. A comparison of the extent of sequential metabolism of *MI* to the extent of metabolism of preformed *MI* showed

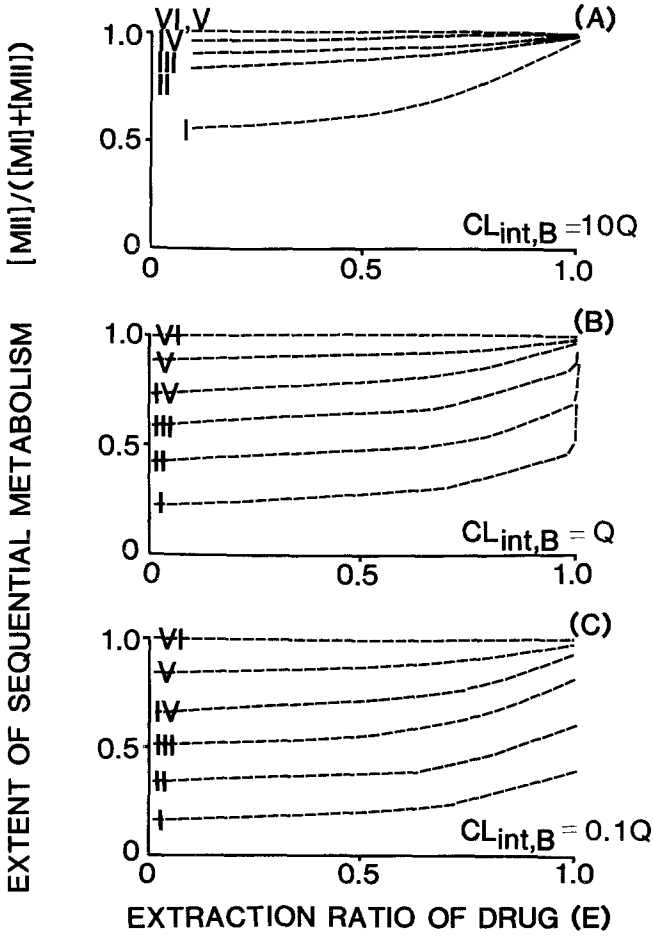

Fig. 5. The relationship between the extent of sequential metabolism of a primary metabolite and the extraction ratio of the parent drug (*E*) when the average hepatic intrinsic clearances for *B* were at (a) 10, (b) 1.0, and (c) 0.1 times hepatic blood flow rate.

again that when the average intrinsic clearances of A and B were high, enzymic distributions were not important (Fig. 5a), but when the average intrinsic clearances of A and B were both intermediate or low (Fig. 5b and c), the extent of sequential metabolism of MI was more sensitive to enzymic distributions.

DISCUSSION

The distribution of hepatic drug metabolizing enzymes in the metabolism of drugs and metabolites has gained considerable attention recently, but the role of enzymic distributions on metabolite kinetics has not been clearly delineated. Simulation studies on enzymic distributions have recently been utilized to predict the outcome of a drug that is competitively metabolized to its conjugates by their respective enzyme systems (27), and the observed data, which were best predicted by the enzymic distribution model, showed that this model is most appropriate. In the description of harmol conjugation, this simulation technique indicates that the sulfotransferases are more abundant in the periportal region, whereas the UDP-glucuronyltransferases are more posteriorly located (24). This method of assigning enzymic distributions for sulfation and glucuronidation reactions reports similar findings to those by Conway *et al.* (28) for the metabolism of hydroxycoumarin to its sulfate and glucuronide conjugates, despite a different technique used.

The present simulation study is aimed at providing an insight into the various distribution patterns and their relative activities so as to understand the efficiency of the organ, given the constraints of these differences in metabolizing a drug and its metabolites. Among the six distribution patterns described, the most efficient model entails that the enzyme for the metabolism of the primary metabolite be present posterior to the enzyme for its formation, and without overlap, to effect efficient metabolism (model VI, Fig. 1). This efficiency is manifested in the extent of sequential metabolism of the (primary) metabolite, which is identical to that of the preformed metabolite. The explanation lies in the full exposure of the primary metabolite to the entire spectrum of metabolic activity of the second enzyme. The least efficient model for enzymic distribution results when the enzymatic activity for the formation of the first metabolite (A) occurs after that for its metabolism (B), and sequential metabolism of this metabolite cannot be effected (reversal of distribution patterns as in model VI, Fig. 1). Among the remaining models, model I proves to be the least efficient, as a majority of the area for activity of enzyme A, the enzyme responsible for formation of the primary metabolite, is present posterior to that for its metabolism, B, and, as a result, sequential metabolism for the primary metabolite may

be handled by the metabolic activity of enzyme *B*, which is present in the region of overlap with enzyme *A* (Fig. 1, model I). When the models are ranked, I to VI proceeds with increasing efficiency for sequential metabolism. The explanation lies with the presence of enzyme *B*, whether before *A* or not, and the region of overlap between the two enzymes.

Interestingly, the distribution of enzyme systems (models I to VI) does not affect the disappearance of the parent compound, as evidenced by the constant value in the extraction ratio for the drug and the preformed metabolite for each given intrinsic clearance. This condition, however, may change when a small diffusion barrier exists for drug and preformed metabolite entry into the eliminating organ, because the transit time and the time of contact between the substrate and the enzyme system may be affected.

The region of least sensitivity of sequential metabolism to enzymic distributions occurs when both the metabolic activities for formation and for metabolism are very high or in a region where hepatic clearance is blood-flow limited (Fig. 2b), while the region of highest sensitivity occurs when both metabolic activities are low (Fig. 5c), because the "effective" activity of the second enzyme depends not only on its intrinsic clearance, but also on the availability of its substrate (primary metabolite), whose presence in the liver depends on the distribution of the two enzyme systems.

Although the simulation study identifies a region of sensitivity (at low average intrinsic clearances of *A* and *B*) to the distribution patterns of the enzymes, this theoretical finding may not operate optimally in a practical setting. Under low metabolic activities of *A* and *B*, it may be difficult to detect the small concentrations of the primary and terminal metabolites formed with sufficient sensitivity to determine the real differences. In this respect, the sensitivity of the extent of metabolism of a metabolite to distribution patterns of the enzymes may be better detected in a system when both the average intrinsic clearances of *A* and *B* (and in particular for *B*) are intermediate. An example of this sensitivity has been displayed in the sequential O-deethylation of phenacetin to acetaminophen and sulfation of acetaminophen to acetaminophen sulfate (14,16,22) and in the metabolic reactions of hydroxylation of acetanilide to acetaminophen and sulfation of acetaminophen to acetaminophen sulfate (22).

REFERENCES

1. S. S. Ketty. Theory and applications of the exchange of inert gas at the lungs and tissues. *Pharmacol. Rev.* **3**:1–41 (1951).
2. M. Gibaldi and D. Perrier. *Pharmacokinetics*, 2nd ed. Marcel Dekker, New York, 1981.
3. K. B. Bischoff and R. L. Dedrick. Thiopental kinetics. *J. Pharm. Sci.* **57**:1346–1351 (1968).

4. K. B. Bischoff, R. L. Dedrick, D. S. Zaharko, and J. A. Longstreth. Methotrexate pharmacokinetics. *J. Pharm. Sci.* **60:**1128–1133 (1971).
5. N. Benowitz, R. P. Forsyth, K. L. Melmon, and M. Rowland. Lidocaine disposition kinetics in monkey and man. I. Prediction by a perfusion model. *Clin. Pharmacol. Ther.* **16:**84–98 (1974).
6. K. Winkler, S. Keiding, and N. Tygstrup. Clearance as a quantitive measure of liver and function. In P. Paumgartner and R. Presig (eds.), *The Liver: Quantitative Aspects of Structure and Functions*, Karger, Basel, pp. 144–155.
7. M. Rowland, L. Z. Benet, and G. G. Graham. Clearance concepts in pharmacokinetics. *J. Pharmacokin. Biopharm.* **1:**123–136 (1973).
8. K. S. Pang and M. Rowland. Hepatic clearance of drugs. II. Experimental evidence for acceptance of the "well-stirred" model over the "parallel tube" model using lidocaine in the perfused rat liver *in situ* preparation. *J. Pharmacokin. Biopharm.* **5:**655–680 (1977).
9. K. S. Pang and M. Rowland. Hepatic clearance of drugs III. Additional experimental evidence for the acceptance of the "well-stirred" model using metabolite (MEGX) data generated from lidocaine under varying hepatic blood flows in the rat liver perfused *in situ* preparation. *J. Pharmacokin. Biopharm.* **5:**681–699 (1977).
10. D. G. Shand, D. M. Kornhauser, and G. R. Wilkinson. Effects of routes of administration and blood flow on hepatic elimination. *J. Pharmacol. Exp. Ther.* **195:**424–432 (1975).
11. S. Keiding, S. Johansen, K. Winkler, K. Tonnesen, and N. Tygstrup. Michaelis-Menten kinetics of galactose elimination in the isolated perfused pig liver. *Am. J. Physiol.* **230:**1302–1313 (1976).
12. S. Keiding and E. Chiarantini. Effect of sinusoidal perfusion on galactose elimination kinetics in perfused rat liver. *J. Pharmacol. Exp. Ther.* **205:**465–470 (1978).
13. S. Keiding, S. Johansen, I. Midtbll, A. Rabol, and L. Christiansen. Ethanol elimination kinetics in human liver and pig liver *in vivo*. *Am. J. Physiol.* **237:**E316–E324 (1979).
14. K. S. Pang and J. R. Gillette. Kinetics of metabolite formation and elimination in the perfused rat liver preparation: differences between the elimination of preformed acetaminophen and acetaminophen formed from phenacetin. *J. Pharmacol. Exp. Ther.* **207:**178–194 (1978).
15. K. S. Pang and J. R. Gillette. Sequential first-pass elimination of a metabolite derived from its precursor. *J. Pharmacokin. Biopharm.* **7:**275–290 (1979).
16. K. S. Pang and J. A. Terrell. Retrogade perfusion to probe the heterogeneous distributions of hepatic drug metabolizing enzymes in the rat. *J. Pharmacol. Exp. Ther.* **216:**339–346 (1981).
17. L. W. Wattenberg and J. L. Leong. Histochemical demonstration of reduced pyridine nucleotide dependent polycyclic hydrocarbon metabolizing systems. *J. Histochem. Cytochem.* **10:**412–420 (1962).
18. J. Baron, J. A. Redick, and F. P. Guengerich. Immunohistochemical localization of cytochromes P-450 in rat liver. *Life Sci.* **23:**2627–2632 (1978).
19. J. H. Dees, B. S. S. Masters, U. Muller–Eberhard, and E. F. Johnson. Effect of 2,3,7,8-tetrachlorodibenzo-p-dioxin and phenobarbital on the occurrence and distribution of four cytochrome P-450 isozymes in rabbit kidney, lung and liver. *Cancer Res.* **42:**1423–1432 (1982).
20. A. E. M. McLean, E. McLean, and J. E. Judah. Cellular necrosis in the liver induced and modified by drugs. *Int. Rev. Exp. Pathol.* **4:**125–157 (1965).
21. J. H. N. Meerman, A. B. van Doorn, and G. J. Mulder. Inhibition of sulfate conjugation of N-hydroxy-2-acetylaminofluorene in isolated perfused rat liver and in the rat *in vivo* by pentachlorophenol and low sulfate. *Cancer Res.* **40:**3772–3779 (1980).
22. K. S. Pang, L. Waller, K. K. Chan, and M. G. Horning. Metabolite kinetics: formation of acetaminophen from deuterated and non-deuterated phenacetin and acetanilide on acetaminophen sulfation kinetics in the perfused rate liver preparation. *J. Pharmacol. Exp. Ther.* **222:**14–19 (1982).
23. K. S. Pang, P. Kong, J. A. Terrell, and R. E. Billings. Disposition of acetaminophen and phenacetin by isolated rat hepatocytes—a system in which the spatial organization inherent of an intact organ is disrupted, submitted for publication.

24. J. R. Gillette. Factors affecting drug metabolism. *Ann. N.Y. Acad. Sci.* **179:**43–46 (1971).
25. G. R. Wilkinson and D. G. Shand. Commentary: A physiological approach to hepatic drug clearance. *Clin. Pharmacol. Ther.* **18:**377–390 (1975).
26. A. A. B. Pritsker. *The GASP IV Simulation Package.* Wiley, New York, 1974.
27. K. S. Pang, H. Koster, I. C. M. Halsema, E. Scholtens, G. J. Mulder, and R. N. Stillwell. Normal and retrograde perfusion to probe the zonal distribution of sulfation and glucuronidation activities of harmol in the perfused rat liver preparation. *J. Pharmacol. Exp. Ther.* **224:**647–653 (1983).
28. J. G. Conway, F. C. Kauffman, S. Ji, and R. G. Thurman. Ratio of sulfation and glucuronidation of 7-hydroxyxoumarin in periportal and pericentral regions of the liver lobule. *Mol. Pharmacol.* **22:**509–516 (1982).